

# BASIC—ALIMENTARY TRACT

## The Epithelial Barrier Is Maintained by In Vivo Tight Junction Expansion During Pathologic Intestinal Epithelial Shedding

AMANDA M. MARCHIANDO,\* LE SHEN,\* W. VALLEN GRAHAM,\* KAREN L. EDELBLUM,\* CARRIE A. DUCKWORTH,<sup>‡</sup> YANFANG GUAN,<sup>§</sup> MARSHALL H. MONTROSE,<sup>§</sup> JERROLD R. TURNER,\* and ALASTAIR J. M. WATSON<sup>||</sup>

\*Department of Pathology, The University of Chicago, Chicago, Illinois; <sup>‡</sup>School of Clinical Sciences, University of Liverpool, Liverpool, England; <sup>§</sup>Department of Molecular and Cellular Physiology, University of Cincinnati, Cincinnati, Ohio; and <sup>||</sup>Norwich Medical School, University of East Anglia, Norwich, England

**BACKGROUND & AIMS:** Tumor necrosis factor (TNF) increases intestinal epithelial cell shedding and apoptosis, potentially challenging the barrier between the gastrointestinal lumen and internal tissues. We investigated the mechanism of tight junction remodeling and barrier maintenance as well as the roles of cytoskeletal regulatory molecules during TNF-induced shedding. **METHODS:** We studied wild-type and transgenic mice that express the fluorescent-tagged proteins enhanced green fluorescent protein–occludin or monomeric red fluorescent protein 1–ZO-1. After injection of high doses of TNF (7.5  $\mu$ g intraperitoneally), laparotomies were performed and segments of small intestine were opened to visualize the mucosa by video confocal microscopy. Pharmacologic inhibitors and knockout mice were used to determine the roles of caspase activation, actomyosin, and microtubule remodeling and membrane trafficking in epithelial shedding. **RESULTS:** Changes detected included redistribution of the tight junction proteins ZO-1 and occludin to lateral membranes of shedding cells. These proteins ultimately formed a funnel around the shedding cell that defined the site of barrier preservation. Claudins, E-cadherin, F-actin, myosin II, Rho-associated kinase (ROCK), and myosin light chain kinase (MLCK) were also recruited to lateral membranes. Caspase activity, myosin motor activity, and microtubules were required to initiate shedding, whereas completion of the process required microfilament remodeling and ROCK, MLCK, and dynamin II activities. **CONCLUSIONS: Maintenance of the epithelial barrier during TNF-induced cell shedding is a complex process that involves integration of microtubules, microfilaments, and membrane traffic to remove apoptotic cells. This process is accompanied by redistribution of apical junctional complex proteins to form intercellular barriers between lateral membranes and maintain mucosal function.**

*Keywords:* Barrier Function; Cell Shedding; Occludin; EGFP; mRFP.

An essential function of the intestine is to maintain a barrier between the gut lumen and internal tissues. A single layer of epithelial cells creates this barrier, and

the space between adjacent epithelial cells is sealed by the tight junction, the principal determinant of barrier function, and the subjacent adherens junction.<sup>1,2</sup> The continual renewal of the surface epithelium, which requires cell shedding, represents a potential site of barrier loss. Although barrier function is maintained during physiologic cell shedding,<sup>3</sup> the risk of gross barrier loss is compounded in inflammatory disease, where epithelial proliferation and turnover are accelerated. Consistent with this, increased tight junction permeability is associated with intestinal disease<sup>2,4,5</sup> and electrical conductance is enhanced directly over sites of epithelial apoptosis.<sup>6</sup> However, although gross barrier function is maintained during shedding,<sup>7</sup> the mechanisms that regulate this process during epithelial turnover are poorly understood.

One mechanism of epithelial cell extrusion that has been proposed on the basis of static images of in vivo intestinal epithelial shedding events involves extension of cytoplasmic processes from adjacent cells beneath the shedding cell.<sup>3</sup> This was suggested to allow adjacent cells to join and seal, like a zipper, from bottom to top during extrusion.<sup>3</sup> Alternatively, in vitro studies of renal epithelia suggest that adjacent cells may simply constrict around an apoptotic cell by mechanisms that involve microfilaments and microtubules as well as rho-associated kinase (ROCK), myosin light chain kinase (MLCK), and p115 RhoGEF.<sup>7,8</sup> The roles of these cytoskeletal structures and regulatory proteins in epithelial extrusion have not been assessed in vivo.

We hypothesized that reorganization of tight junction proteins might be an essential component of epithelial extrusion and barrier maintenance. To assess this, we used the pathophysiologically relevant model of intestinal epithelial cell shedding induced by administration of high-dose tumor necrosis factor (TNF) and in vivo im-

*Abbreviations used in this paper:* EGFP, enhanced green fluorescent protein; MLC, myosin light chain; MLCK, myosin light chain kinase; mRFP1, monomeric red fluorescent protein 1; ROCK, Rho-associated kinase; TNF, tumor necrosis factor.

© 2011 by the AGA Institute  
0016-5085/\$36.00  
doi:10.1053/j.gastro.2011.01.004

aging of mice expressing fluorescent-tagged tight junction proteins.<sup>4</sup> Redistribution of ZO-1 and occludin from the apical junctional complex to lateral membranes was the first detectable event in TNF-induced shedding. Progression of extrusion was characterized by luminal movement and constriction of this funnel, which defined the site of barrier preservation. Other tight and adherens junction proteins, actin, myosin, and the critical regulators ROCK and MLCK were also recruited to lateral membrane funnels. Shedding could be largely blocked by inhibition of caspase cleavage, microfilament and microtubule remodeling, myosin II motor activity, ROCK, MLCK, or dynamin. However, these agents affected different stages of extrusion, indicating that each has specific roles in this process. These data show that apoptotic shedding involves redistribution of junctional proteins along lateral membranes by a process that requires cytoskeletal remodeling and membrane trafficking events to complete extrusion and maintain barrier function.

## Materials and Methods

### Animals

Seven- to 10-week old C57BL/6 wild-type, transgenic, and 210-kilodalton MLCK<sup>-/-</sup> mice were housed in an Association for Assessment and Accreditation of Laboratory Animal Care-accredited facility using Institutional Animal Care and Use Committee-approved procedures, as described.<sup>4,9</sup>

### Live Animal Imaging

Imaging of anesthetized animals was performed as previously described (Supplementary Materials and Methods).<sup>4,10</sup> Inhibitors were perfused luminally for 1 hour before imaging.

### Immunofluorescence

Images of immunostained sections were obtained, and deconvolved z-stacks were used to assess the number of shedding cells (Supplementary Materials and Methods). Twenty fields from each of 2 mice were counted for each condition. Results were normalized to the length of basement membrane, and at least 60,000  $\mu\text{m}$  was examined for each condition.

### Statistical Analysis

Data are presented as means  $\pm$  SEM for at least 3 independent experiments.

## Results

### Barrier Function Is Maintained During TNF-Induced Cell Shedding

To visualize shedding in intact epithelia, in vivo imaging of wild-type mice was performed as described previously.<sup>4,11</sup> Only rare shedding events followed administration of low-dose (5  $\mu\text{g}$ ) TNF, which causes tight

junction barrier loss and water secretion.<sup>4,9</sup> In contrast, high-dose (7.5  $\mu\text{g}$ ) TNF induced abundant epithelial shedding beginning 90 minutes after administration ( $6.2 \times 10^{-3} \pm 4.7 \times 10^{-3}$  events/mm basement membrane at 120 minutes). Neighboring cells shed in rapid succession in some areas, and this continued to the end of the experiment (180 minutes after TNF) (Figure 1A and Supplementary Video 1). However, the barrier to small hydrophilic solutes was maintained (Figure 1A and B). Extracellular calcium chelation confirmed sensitivity of the barrier detection method and requirement for adherens and tight junctions in barrier maintenance (Figure 1C).

Morphologic changes typical of apoptosis were not apparent until the nucleus of the shedding cell had moved above the nuclei of adjacent cells, at which point chromatin fragmentation and condensation began (Figure 1A and B). Only apically oriented shedding was detected in more than 1500 events; basally oriented shedding was not observed.

### Perijunctional Actin Is Remodeled During Cell Shedding

Extrusion of apoptotic cells requires actin polymerization as well as ROCK and MLCK activity in vitro.<sup>7</sup> To preliminarily assess the role of actomyosin during in vivo epithelial extrusion, sections were harvested 120 minutes after administration of high-dose TNF and labeled to detect F-actin and nuclei. Comparison with live imaging data permitted identification of shedding cells and 3 patterns of microfilament reorganization associated with this process (Figure 1D). Microfilaments extended along basolateral membranes of some cells to outline a saccular epithelial shape. In other cases, lateral membranes were more rigid, consistent with the development of tension, and formed a funnel that surrounded the extruding cell. Finally, microfilaments formed a "V" shape, sometimes with an extended apex, surrounding cells in which the nucleus was significantly displaced above those of adjacent cells.

### ZO-1 and Occludin Are Actively Redistributed During Epithelial Shedding

To determine whether ZO-1 is redistributed during in vivo extrusion, neurovascularly intact jejunal mucosa of transgenic mice expressing either enhanced green fluorescent protein (EGFP)-occludin or monomeric red fluorescent protein 1 (mRFP1)-ZO-1 fusion proteins within intestinal epithelia<sup>4</sup> were studied between 90 and 180 minutes after administration of 7.5  $\mu\text{g}$  TNF (Figure 2). In these mice, mRFP1-ZO-1 is specifically associated with the tight junction, whereas overexpression causes EGFP-occludin to be distributed at the tight junction and along lateral membranes.<sup>4</sup> Approximately 2 minutes before the nucleus began to move apically, ZO-1 migrated downward along lateral membranes, completely covering the basolateral surface (Figure 2A and B). Con-

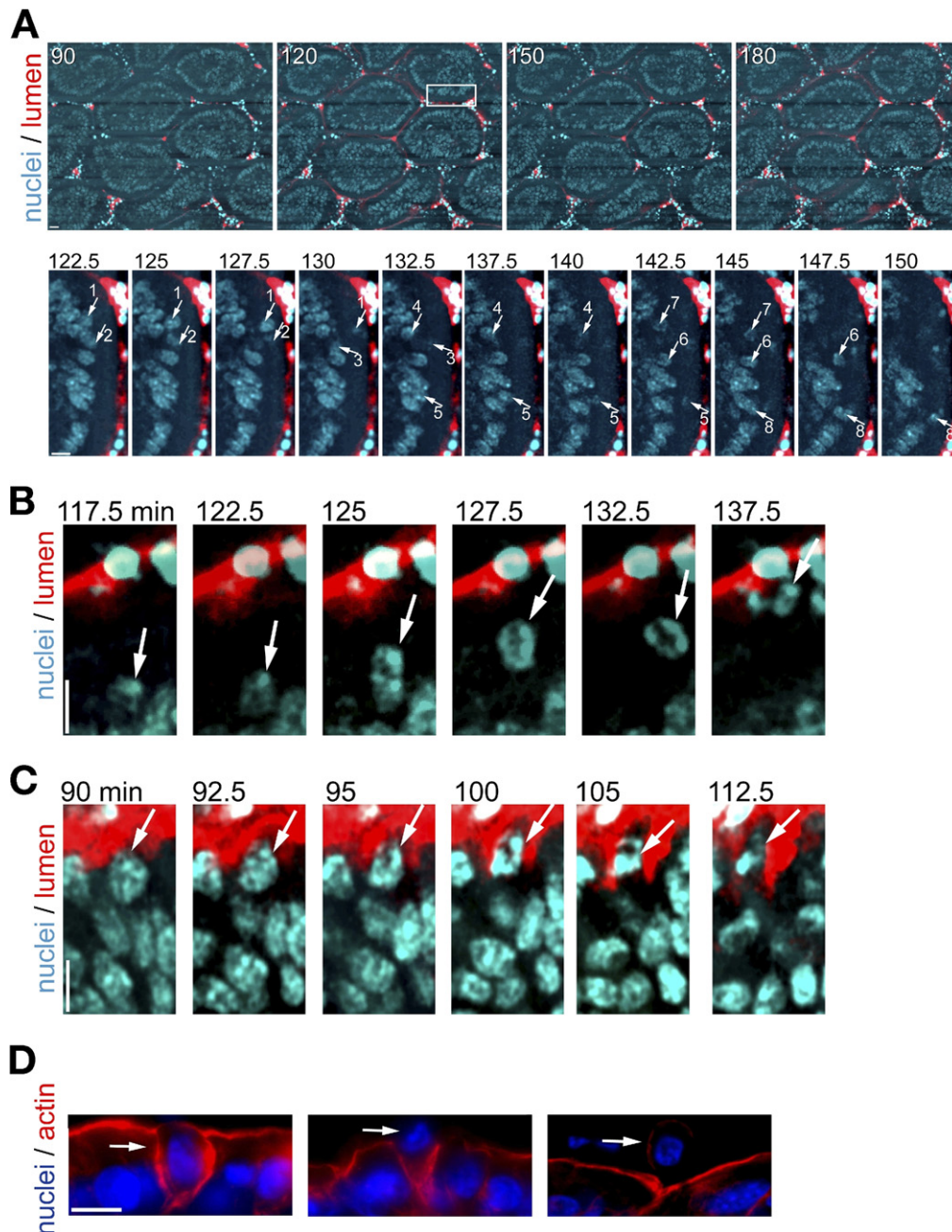


**Figure 1.** High-dose TNF increases cell shedding but does not compromise barrier function. (A, upper panel) In vivo imaging of cell shedding in wild-type mice. Low-magnification time-lapse images at indicated times after administration of 7.5  $\mu\text{g}$  TNF. Bar = 20  $\mu\text{m}$ . Time after administration of TNF (in minutes) is indicated on the images. Nuclei were labeled with Hoechst 33342. Alexa 633 (1  $\mu\text{g}/\text{mL}$ ) was used as a luminal permeability marker (red). (A, lower panel) Zoomed views show a time lapse of shedding events. Bar = 10  $\mu\text{m}$ . (B) High-magnification time-lapse images of a single shedding event. Bar = 10  $\mu\text{m}$ . (C) High-magnification time-lapse images of a single shedding event after administration of EDTA. Bar = 10  $\mu\text{m}$ . (D) Fixed tissue sections of jejunum from wild-type mice 120 minutes after administration of 7.5  $\mu\text{g}$  TNF; F-actin (red) and nuclei (blue). Bar = 10  $\mu\text{m}$ .

sistent with the microfilament redistribution detected in fixed tissues, this initially defined a loose saccular shape (Figure 2B, 5 minutes after commencement of cell shedding). Coincident with apical nuclear movement, the lateral membranes became rigid and formed a funnel (Figure 2B, 7.5 minutes). Further contraction allowed this funnel to be converted to a “V” shape (Figure 2B, 10 minutes). Ultimately, the monolayer was entirely repaired

(Figure 2B, 20 minutes), with complete expulsion of the shed nucleus into the lumen, movement of adjacent nuclei to fill the vacated position within the monolayer, and removal of basolateral membrane-associated mRFP1-ZO-1 (Supplementary Video 2). The entire process required 20 minutes or less in 86% of cases ( $n = 137$  shedding events). EGFP-occludin was similarly redistributed during epithelial shedding (Figure 2A and C and

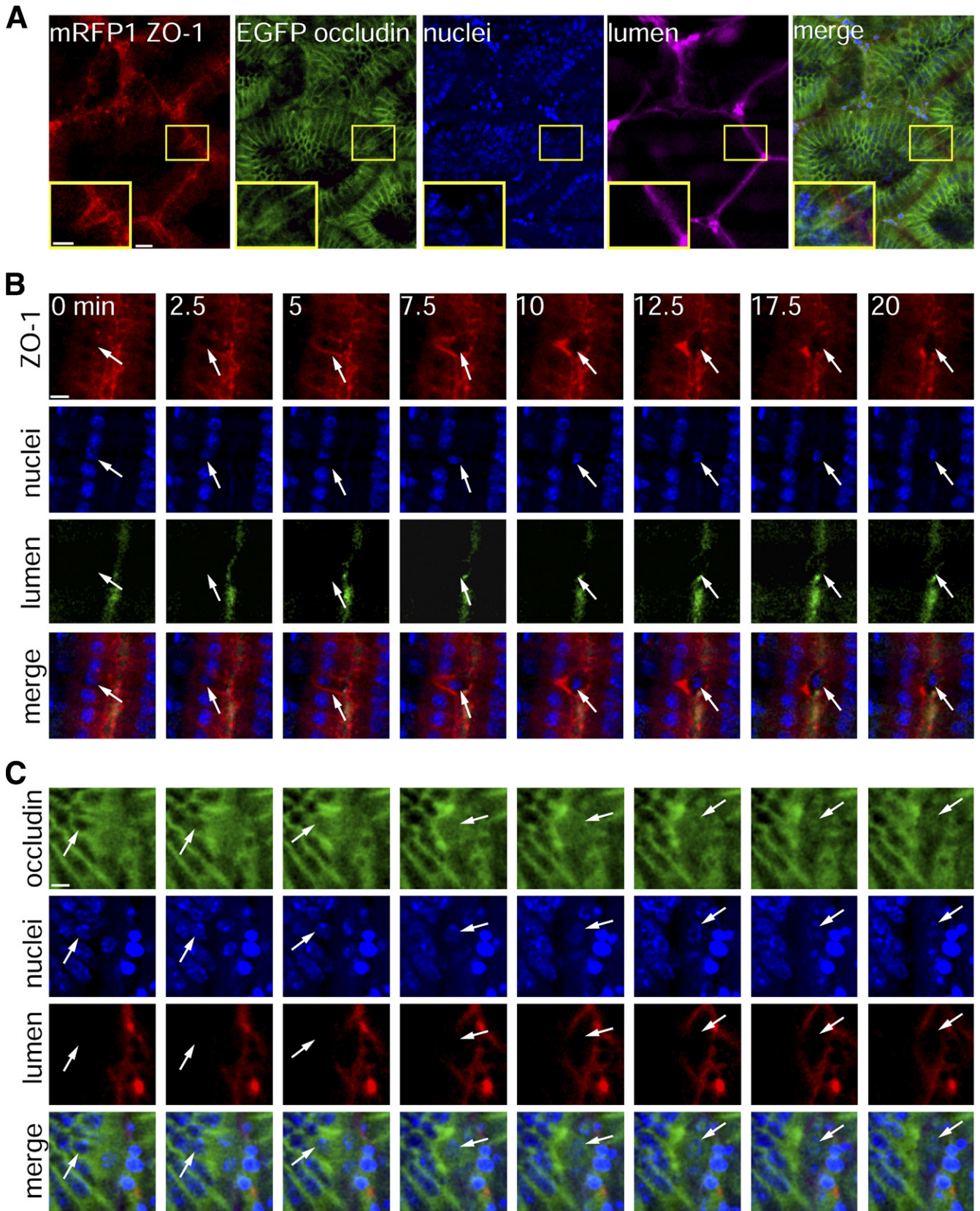


**Figure 2.** Tight junction proteins are remodeled during cell shedding. (A) In vivo imaging of EGFP-occludin and mRFP1-ZO-1 during cell shedding in transgenic mice after administration of 7.5  $\mu\text{g}$  TNF. Bar = 20  $\mu\text{m}$ ; zoomed views bar = 10  $\mu\text{m}$ . (B and C) High-magnification time-lapse images of (B) mRFP1-ZO-1 (red) and (C) EGFP-occludin (green) redistribution during a single shedding event. The luminal dye is 1  $\mu\text{g}/\text{mL}$  Alexa 633. Bars = 10  $\mu\text{m}$ .

Supplementary Video 3). Moreover, similar redistribution of endogenous ZO-1 and occludin was identified by immunofluorescence of tissues from TNF-treated wild-type mice (not shown), showing that the events observed are not artifacts of protein overexpression or the fluorescent tag.

The live imaging data indicate that the epithelial barrier is maintained during TNF-induced shedding. Further examination indicated that the apical limit of mRFP1-ZO-1 and EGFP-occludin, which colocalized with one another (Figure 2A), also marked the site of the barrier to luminal solute permeation (Figure 2A-C). Thus, together with the demonstration that disruption of tight junctions by calcium chelation<sup>12</sup> induced paracellular dye leakage (Figure 1C), these data suggest the tight junction contributes to barrier maintenance during epithelial extrusion.

### ***The Apical Junctional Complex Is Remodeled During Epithelial Shedding***

ZO-1 and occludin are important to tight junction assembly and maintenance,<sup>4,13,14</sup> but claudin proteins are required for paracellular barrier function.<sup>15</sup> Consistent with ZO-1 and occludin reorganization, claudin-7 and claudin-15 were redistributed over lateral membranes as shedding occurred (Figure 3A). Similarly, although E-cadherin is normally present at the lateral membrane, this pool was enriched along lateral membranes of shedding cells (Figure 3A, untreated tissue; Supplementary Figure 1).

Recent work has shown a critical role for vesicular traffic during in vivo tight junction regulation by TNF.<sup>4</sup> We therefore hypothesized that membrane traffic might facilitate cell shedding and redistribution of tight junction proteins. To assess this, jejunum were perfused with dynasore, a specific dynamin inhibitor.<sup>16</sup> Dynasore prevented 65% of shedding events ( $P < .01$ ) (Figure 3B), suggesting a role for dynamin II-dependent membrane traffic during in vivo epithelial shedding. Moreover, in vivo imaging showed, after initiation, that shedding events froze and the funnels observed were maintained without progression for up to 90 minutes (not shown).

### ***Microfilaments and Microtubules Both Contribute to Epithelial Shedding In Vivo***

The apical junctional complex is structurally and functionally linked to the perijunctional actomyosin ring. To preliminarily determine whether actin regulatory proteins contribute to shedding, distributions of ROCK and MLCK, as well as myosin II heavy chains and serine-19 phosphorylated myosin II regulatory light chain (MLC), were assessed (Figure 3A, untreated tissue; Supplementary Figure 1). ROCK is normally present throughout the cytoplasm but was concentrated at lateral membranes during shedding. Similarly, MLCK, which normally localizes to the perijunctional actomyosin ring,

extended to lateral membranes of shedding cells. Consistent with the activities of these kinases,<sup>17</sup> extrusion was associated with increased MLC phosphorylation along rigid, but not saccular, lateral membranes. Whereas myosins IIA, IIB, and IIC are all expressed in cancer-derived intestinal epithelial cell lines,<sup>18</sup> only IIA and IIC were detected in jejunal villous enterocytes (Figure 3A and Supplementary Figure 1). Myosin IIA was normally distributed in punctate foci throughout the cytoplasm but was also found in punctate along the lateral membranes of shedding cells. In contrast, myosin IIC was predominantly localized to the perijunctional actomyosin ring, suggesting that, in contrast to in vitro studies,<sup>18</sup> this isoform may regulate the apical junction complex in vivo. Consistent with that hypothesis, myosin IIC was redistributed along lateral membranes of shedding cells.

As a whole, these data suggest that microfilaments and their regulators contribute significantly to epithelial shedding in vivo. To explore this further, inhibitors of actomyosin function were perfused through jejunum of mice treated with high-dose TNF. Consistent with in vitro data, cytochalasin D potently inhibited in vivo epithelial shedding, preventing 60% of shedding events ( $P < .01$ ) (Figure 3B). Similarly, the myosin II motor inhibitor blebbistatin<sup>19</sup> and the rho kinase inhibitor Y27632<sup>20</sup> strongly inhibited in vivo epithelial shedding, preventing 86% and 67% of shedding events ( $P < .01$ ), respectively (Figure 3B). Shedding was also assessed in long MLCK<sup>-/-</sup> mice, the only isoform expressed in intestinal epithelia.<sup>9,21</sup> TNF-induced shedding was reduced by 87% in these mice ( $P < .01$ ) (Figure 3B). In vivo analysis showed that cytochalasin D, blebbistatin, Y27632, and long MLCK<sup>-/-</sup> slowed, but did not prevent, progression of shedding events (not shown), suggesting the existence of escape pathways.

A recent report has indicated a significant role of tubulin in defining the polarity of apoptotic cell shedding in vitro.<sup>8</sup> Consistent with a role for microtubules during in vivo shedding, tubulin was distributed continuously along lateral membranes of shedding cells in a manner similar to actin and other proteins (Figure 3A). Moreover, colcemid prevented 85% of shedding events (Figure 3B). However, even in colcemid-treated mice, only apically oriented funnels and cell extrusion were observed.

### ***Epithelial Shedding Requires Caspase Cleavage***

The relative roles of apoptosis and anoikis in intestinal epithelial shedding are unclear.<sup>10,22,23</sup> Immunofluorescent staining showed a punctate distribution of cleaved caspase-3 within the cytoplasm of shedding cells, suggestive of activation around mitochondria, but this was only detectable after other features of cell shedding were evident (Figure 3A). To test whether caspase cleavage is required for the initiation of TNF-induced cell shedding, jejunum of TNF-treated mice were

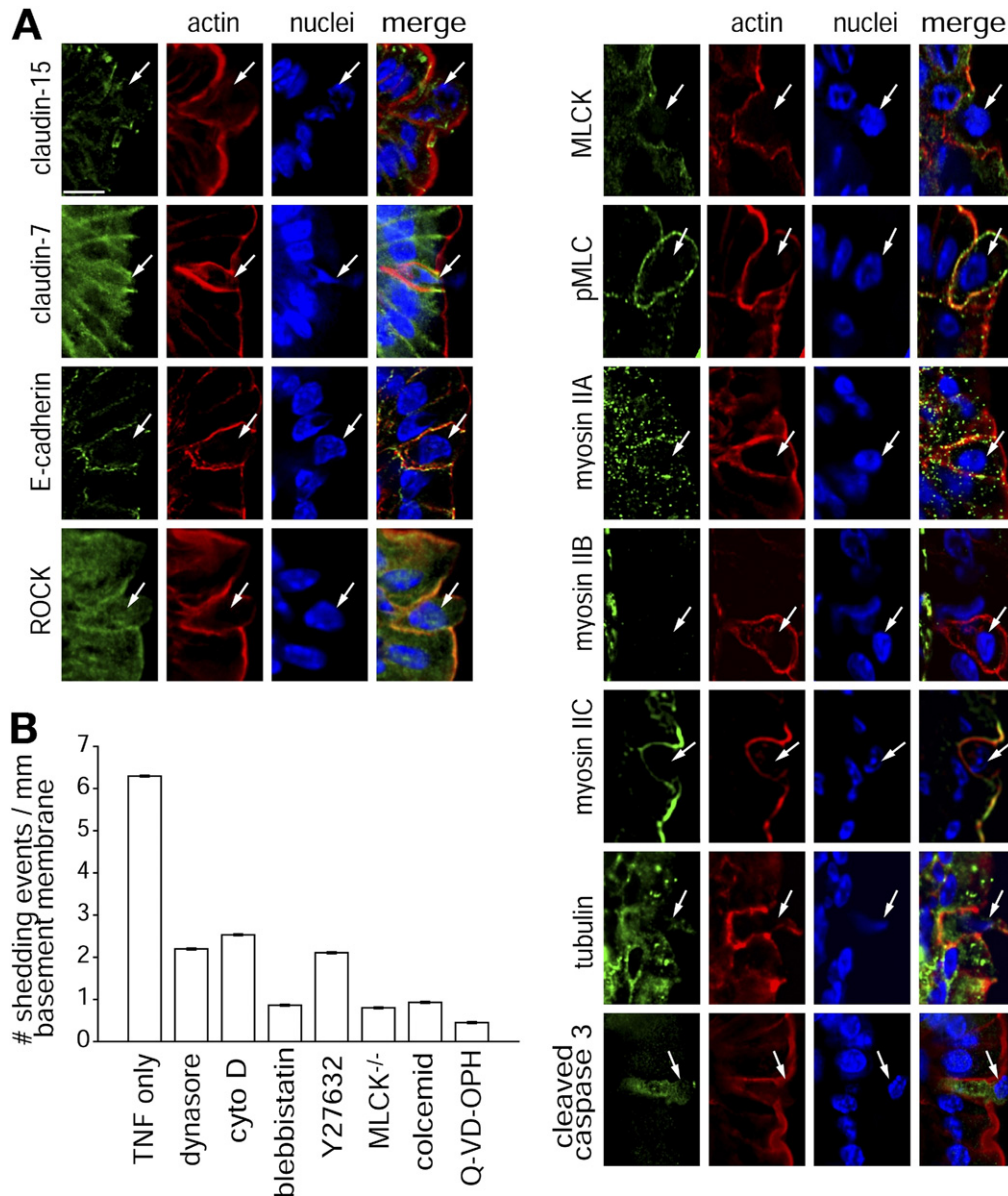


**Figure 3.** Proteins are remodeled in shedding cells. (A) Jejunum was harvested from wild-type mice 120 minutes after intraperitoneal injection of 7.5  $\mu\text{g}$  TNF and labeled for claudin-15, claudin-7, E-cadherin, ROCK, MLCK, phosphorylated MLC (pMLC), myosin IIA, myosin IIB, myosin IIC, cleaved caspase 3, tubulin (green), F-actin (red), and nuclei (blue). Arrows indicate the nucleus of shedding cell. Bar = 10  $\mu\text{m}$ . (B) Wild-type mice were injected with 7.5  $\mu\text{g}$  TNF, and a segment of jejunum was perfused with 50  $\mu\text{mol/L}$  dynasore, 40  $\mu\text{mol/L}$  cytochalasin D, 500  $\mu\text{mol/L}$  blebbistatin, 400  $\mu\text{mol/L}$  Y27632, 400  $\mu\text{mol/L}$  colcemid, 50  $\mu\text{mol/L}$  Q-VD-OPH, or isotonic solution. MLCK<sup>-/-</sup> mice were injected with 7.5  $\mu\text{g}$  TNF and a segment of jejunum perfused with isotonic solution. Jejunum was harvested 120 minutes after TNF and labeled for ZO-1 (green), F-actin (red), and nuclei (blue). The number of shedding events was counted in at least 60,000  $\mu\text{m}$  of basement membrane per condition.

perfused with Q-VD-OPh, a potent, broad-spectrum caspase inhibitor.<sup>24</sup> This blocked 93% ( $P < .01$ ) of shedding events. These data suggest that caspase cleavage is necessary for TNF-induced cell shedding to occur. However, because MLC phosphorylation occurred normally in the few events that did occur after Q-VD-Oph perfusion (Figure 3B and Supplementary Figure 2), the results indicate that either caspase inhibition was incomplete or escape mechanisms that do not require caspase cleavage exist.

### Cell Shedding Occurs via an Ordered Series of Events

Live imaging suggests that TNF-induced shedding occurs in a reproducible, stepwise process (Figure 4). To understand this better, tissues were examined by transmission electron microscopy (Figure 4A). The first recognizable event was reorganization of ZO-1, occludin, and F-actin along the lateral membranes (Figure 4B). This was accompanied by partial microvillus vesiculation and intracellular

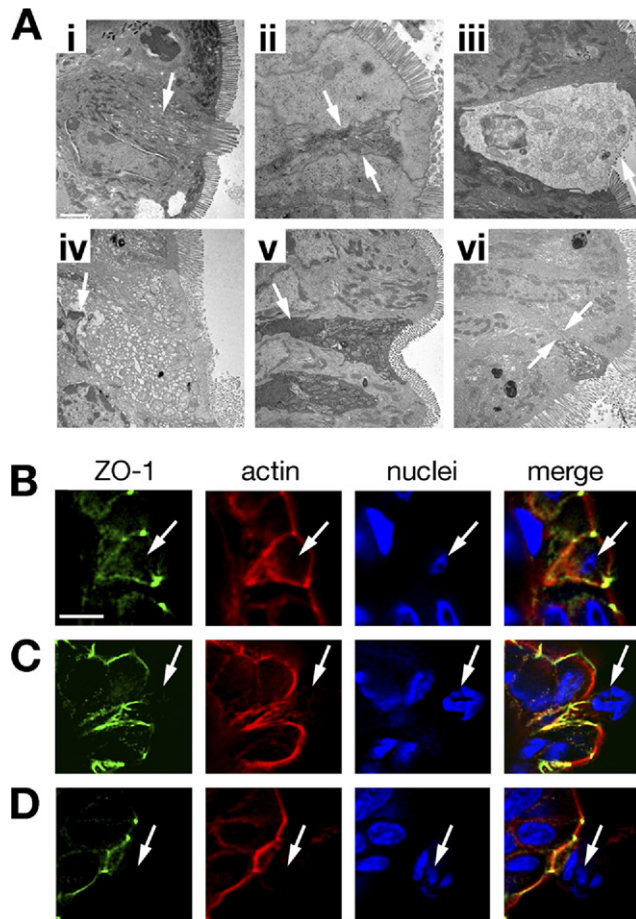


**Figure 4.** Cell shedding can be defined by early, middle, and late stages. (A) Electron micrographs of aldehyde-fixed, plastic-embedded jejunum harvested from wild-type mice 120 minutes after TNF injection. As shedding progressed, organelles broke down (arrow in *i* and *ii*), cells assumed a funnel shape (arrow indicates lateral membrane of shedding cell in *ii*), and microvilli vesiculated (arrow in *iii*). Nuclei of shedding cells condensed and fragmented (arrow in *v*), and the nuclear envelope became indistinct (arrow in *iv*). Neighboring cells filled the space left by the shedding cell from beneath (arrows in *vi*). (B–D) Jejunum was harvested from wild-type, mRFP1–ZO-1, or EGFP–occludin mice 120 minutes after administration of 7.5  $\mu$ g TNF intraperitoneally and labeled for ZO-1 (red) and F-actin (green) or occludin (green) and F-actin (red). Nuclei are blue. (B) Early-stage cell shedding. (C) Middle-stage cell shedding. (D) Late-stage cell shedding. Bar = 10  $\mu$ m.

organelle breakdown (Figure 4A). This progressed to an intermediate stage within 5 minutes and was characterized by rigidity of lateral membranes (Figure 4C), complete vesiculation of microvilli, early nuclear condensation, and nuclear envelope fragmentation (Figure 4A). Terminal contraction of surrounding epithelia completed extrusion, and the monolayer was resealed during the final stage (Figure 4D).

#### **Apoptotic, Cytoskeletal, and Membrane Traffic Inhibition Interfere With Distinct Stages of Epithelial Shedding**

To determine the stage at which inhibitors blocked shedding, the proportion of identified events in

each stage was assessed. Without inhibitors, 89% of detected shedding events were late stage and only 11% were early or middle stage (Figure 5A). In contrast, 28% and 29% of events were early or middle stage, respectively, after Q-VD-OPH treatment (Figure 5A and B). Together with the overall inhibition of shedding, these data suggest that caspase activation is required for initiation and progression of this process.

Microtubule polymerization also appeared to be essential for early stages of shedding and subsequent extrusion (Figure 5A and B). After colcemid treatment, 52% of detected shedding events were early stage and only 35% were late stage. However, events that were initiated were ultimately completed, indicating that either alternative mechanisms or residual colcemid-resistant microtubules can compensate, albeit inefficiently, for generalized microtubule loss.

The myosin II motor inhibitor blebbistatin markedly inhibited progression of cell shedding, with 66% of observed events in the earliest stages (Figure 5A and B). This suggests that actomyosin contraction is required for development of tension along lateral membranes and for progression from early to middle stages. Actin depolymerization, ROCK inhibition, and long MLCK knockout also increased the proportion of shedding events in early stages, as well as those in middle stages to 47% after cytochalasin D treatment, 48% after Y27632 treatment, and 54% in MLCK<sup>-/-</sup> mice, respectively (Figure 5A and B). Moreover, when late-stage events were identified in these conditions, they tended to be arrested. This was most obvious in Y27632-treated tissues (Figure 5B).

Dynasore had the most profound effect on TNF-induced epithelial shedding. Many partially extruded cells accumulated (Figure 5C) and persisted for up to 60 minutes, with the majority (66%) trapped in early or middle stages of shedding (Figure 5A and B). Despite this paralysis, the barrier was maintained at these sites (Figure 5C). Thus, dynamin plays a critical role in progression of the shedding process from early to middle as well as middle to late stages but is not required for barrier maintenance.

## **Discussion**

Epithelial extrusion occurs millions of times each day in the mammalian intestine. The frequency of such events is further amplified in inflammatory disease, where epithelial turnover occurs at significantly increased rates. Barrier defects associated with epithelial extrusion have been implicated as a cause of the barrier dysfunction associated with enterocolitis in experimental models and patients with inflammatory bowel disease<sup>6,25</sup> and may even be sites of pathogen entry.<sup>26</sup> Despite these defects, the epithelial barrier remains largely intact, even in the face of extensive shedding. The goal of these studies was to identify the mechanisms that maintain the epithelial barrier during pathologic cell shedding.

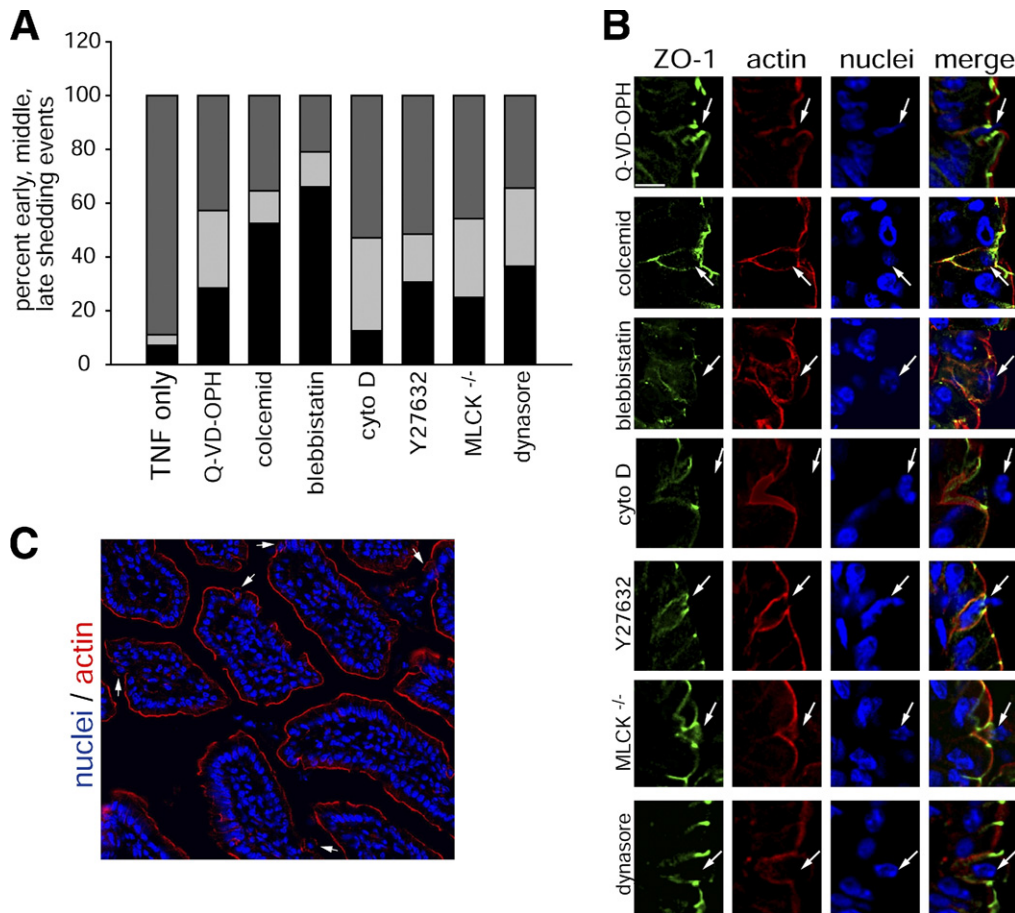


**Figure 5.** Extrusion of apoptotic shedding cells requires cytoskeletal elements and membrane traffic. (A) Wild-type mice were injected with 7.5  $\mu\text{g}$  TNF, and a segment of jejunum was perfused with 50  $\mu\text{mol/L}$  Q-VD-OPH, 400  $\mu\text{mol/L}$  colcemid, 500  $\mu\text{mol/L}$  blebbistatin, 40  $\mu\text{mol/L}$  cytochalasin D, 400  $\mu\text{mol/L}$  Y27632, 50  $\mu\text{mol/L}$  dynasore, or isotonic solution. MLCK<sup>-/-</sup> mice were injected with 7.5  $\mu\text{g}$  TNF, and a segment of jejunum was perfused with isotonic solution. Jejunum was harvested 120 minutes after administration of TNF and labeled for ZO-1 (green), F-actin (red), and nuclei (blue). At least 60,000  $\mu\text{m}^2$  of basement membrane was examined per condition. The stages of cell shedding were determined by F-actin and ZO-1 staining as in Figure 4B–D. The percentage of events observed in each stage of shedding varied between the inhibitors used. (B) Remodeling of ZO-1 (green) and F-actin (red) along lateral membranes of shedding cells in wild-type mice after perfusion with Q-VD-OPH, colcemid, blebbistatin, cytochalasin D, Y27632, and dynasore and in MLCK<sup>-/-</sup> mice. Arrows indicate nucleus of shedding cell. (C) A segment of jejunum was perfused with 50  $\mu\text{M}$  dynasore for 60 minutes before injection of 7.5  $\mu\text{g}$  TNF. Tissue was harvested 120 minutes after TNF injection and labeled for F-actin (red) and nuclei (blue). Low-magnification images show an accumulation of partially extruded cells (arrows). Bar = 10  $\mu\text{m}$ .

Increased rates of intestinal epithelial shedding are commonly associated with increased mucosal TNF production and can be reduced by TNF neutralization.<sup>27</sup> This suggests that TNF-induced cell shedding is a pathophysiologically relevant model of accelerated cell turnover. We took advantage of recently developed techniques and transgenic mice to study *in vivo* shedding by video confocal microscopy. The data reveal a remarkable redistribution of ZO-1 and occludin, from the tight junction to basolateral membranes, where they define the site of barrier maintenance. Claudins, E-cadherin, tubulin, F-actin, ROCK, and MLCK are also recruited to basolateral membranes, where contraction results in development of a funnel that appears to expel the apoptotic cell. We further showed essential roles for actomyosin contraction, microtubule remodeling, intracellular cytoskeletal regulators, and dynamin II. Taken as a whole, the data

show that tight and adherens junction-like structures assemble over the lateral membranes to maintain the barrier between shedding and adjacent healthy epithelial cells.

Although our data are the first to examine tight junction reorganization during pathologic cell shedding *in vivo*, an elegant 1990 study by Madara reported proliferation of tight junction-like strands along lateral membranes of small intestinal epithelia undergoing spontaneous, homeostatic shedding.<sup>3</sup> The presence of strands at these sites is consistent with our observation that claudin proteins are recruited to basolateral membranes. Moreover, although the available technology limited the previous study to static images of shedding events, Madara was able to show that diffusion of a soluble luminal tracer, horseradish peroxidase, was restricted at the apical site at which these irregular junctional strands were

found. Thus, although the methods used were very different, the previous ultrastructural data and our live imaging data are comparable in their demonstration of widespread tight junction assembly along lateral membranes of shedding intestinal epithelial cells. Although the limitation of static images prevented Madara from measuring the rate at which these structures formed and sealed potential gaps left by cells being shed spontaneously, we were able to determine that, in the majority of cases, TNF-induced shedding and resealing required less than 20 minutes. This is also consistent with our recent data (Guan et al, manuscript in submission) showing that discontinuities, or gaps,<sup>10,11</sup> left after spontaneous shedding resolve rapidly (<10 minutes), with the epithelium returning to basal state within 20 minutes.

There has been considerable debate as to whether intestinal epithelial shedding is initiated by apoptosis or, alternatively, apoptosis is triggered by shedding (ie, anoikis) *in vivo*.<sup>10,22,23,28</sup> We found that caspase-3 was undetectable until after other features of cell shedding were evident (Figure 3A). This suggests that caspase-3, an essential element of both intrinsic and extrinsic apoptotic pathways, may be activated after initiation of cell shedding and is consistent with the observation that the less specific, and more toxic, caspase inhibitor ZVAD-fmk does not prevent *in vitro* shedding.<sup>7</sup> However, we were able to inhibit *in vivo* shedding with the general caspase inhibitor Q-VD-OPH (Figure 3B).<sup>24</sup> Furthermore, the few cells that started to shed in the presence of Q-VD-OPH were in early or middle stages, whereas an overwhelming majority of events were of late stage in the absence of Q-VD-OPH (Figure 5A and B). Consistent with this observation, caspase inhibition did not prevent MLC phosphorylation, suggesting that caspases are acting distal to events that activate MLC phosphorylation, that MLC phosphorylation and caspase cleavage are on separate pathways, or that there is an escape mechanism that can overcome caspase inhibition. These data also suggest that caspase cleavage precedes shedding and that our failure to detect caspase-3 cleavage until after shedding reflects limited sensitivity of the approach. Alternatively, the effect of Q-VD-OPH may partly reflect inhibition of other caspases, because caspase-3 activation is normally a late event in apoptosis. In either case, these data argue strongly that TNF-induced cell shedding is triggered by caspase activation rather than epithelial detachment, indicating that the process is one of apoptosis and not anoikis.

In contrast to previous studies of spontaneous shedding, we did not identify long-lived gaps after TNF-induced shedding. This suggests that, despite similarities, physiologic and pathologic cell shedding are distinct processes. This conclusion is further supported by the observation that TNF-induced shedding is markedly decreased in long MLCK<sup>-/-</sup> mice. Because basal intestinal morphology is unremarkable in these mice, spontaneous,

or homeostatic, shedding must proceed normally by a long MLCK-independent mechanism in these mice. This does not, however, exclude a role for MLC phosphorylation and actomyosin contraction in spontaneous shedding, because basal intestinal epithelial MLC phosphorylation is similar in long MLCK<sup>-/-</sup> and wild-type mice.<sup>9</sup> This mechanism may also be responsible for the inefficient completion of TNF-induced cell shedding in MLCK<sup>-/-</sup> mice. Moreover, as long MLCK<sup>-/-</sup> mice fail to internalize occludin and develop barrier defects following treatment with low-dose TNF<sup>9</sup> (high-dose TNF does induce some shedding), TNF-induced tight junction regulation and epithelial shedding are distinct, separable processes. Although not addressed here, these stark differences between low-dose and high-dose TNF may relate to differing affinities of the 2 TNF receptors. TNFR2, which regulates tight junction permeability,<sup>29</sup> has a high affinity for TNF (ie, is activated by low doses),<sup>30</sup> whereas TNFR1 requires higher TNF concentrations to induce epithelial apoptosis.<sup>31</sup>

It is not surprising that actomyosin contraction contributes to *in vivo* shedding, because actin remodeling, ROCK, and MLCK are involved in MDCK cell extrusion.<sup>7</sup> Moreover, microtubules have been previously implicated in MDCK cell shedding<sup>7</sup> and closure of plasma membrane wounds,<sup>32</sup> perhaps because microtubules can serve to organize microfilament assembly and recruit myosin II to wound edges. However, despite recent data suggesting that microtubules determine the polarity of MDCK cell extrusion *in vitro*,<sup>8</sup> we did not find any examples of basal extrusion, even in the presence of colcemid. This may reflect anatomic differences between *in vitro* and *in vivo* situations, such as the presence of a basement membrane in the latter.

The rapidity with which occludin, claudins, and E-cadherin, all of which are transmembrane proteins, spread over basolateral membranes is remarkable. Although vesicular traffic could be responsible for this redistribution, membrane traffic has not been previously implicated in epithelial shedding, *in vitro* or *in vivo*. We found that dynasore, a specific inhibitor of dynamin, markedly inhibited shedding. Moreover, the few shedding events present were trapped in early and middle stages. This may reflect other roles of dynamin, including interactions mediated by Tuba,<sup>33</sup> a Cdc42 GEF that can regulate microfilament assembly and stability in nonepithelial cells. However, the markedly different effects of cytochalasin and dynasore argue that the latter is more likely to reflect inhibition of vesicular traffic. Thus, although further analysis is necessary, these data are the first to indicate a potential role for dynamin II-dependent membrane traffic in epithelial shedding.

Overall, the data suggest a model for the process of *in vivo* TNF-induced cell shedding in which epithelial apoptosis is initiated before morphologically recognizable changes (Figure 6). This proceeds to early stages of shedding in

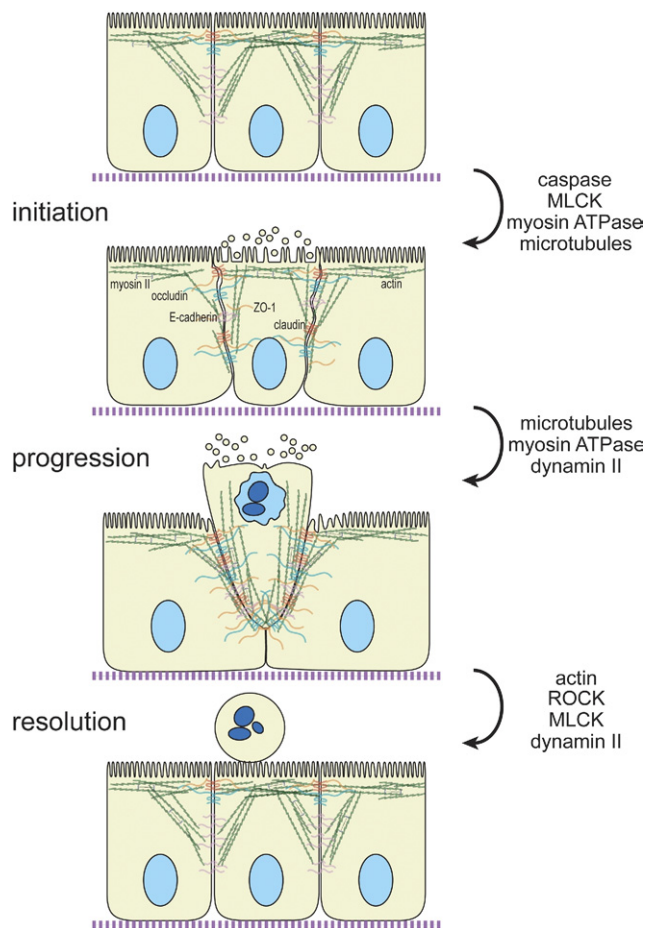


**Figure 6.** A model for the mechanism of TNF-induced intestinal epithelial extrusion. Caspase cleavage is required to initiate the process, with additional contributions from MLCK and myosin adenosine triphosphatase activity as well as microtubule-dependent events. This is followed by redistribution of cytoskeletal, tight junction, and adherens junction proteins along lateral membranes of cell that will be shed. Myosin adenosine triphosphatase activity and both microtubule- and dynamin-dependent events are required for development of tension along lateral membranes and progression of extrusion. Finally, adjacent cells move into, and beneath, the space left by the shedding cell. This resolution requires actin reorganization, ROCK, MLCK, and dynamin.

which tight and adherens junction and cytoskeletal proteins reorganize along basolateral membranes to expand the scope of the paracellular barrier. Myosin II motor activity and microtubule remodeling cause contraction of the shedding cell and its neighbors, resulting in development of tension along the lateral membranes. In contrast to previous models in which adjacent cells migrate beneath the shedding cell,<sup>3</sup> our data suggest that attachments between shedding and adjacent cells are maintained during extrusion as a result of the expanded distribution of junctions along basolateral membranes. ROCK, MCLK, and dynamin II direct further contraction and membrane flow until extrusion is complete. New junctions are formed between adjacent cells as the shedding cell leaves the monolayer, possibly by mechanisms that involve ROCK, MCLK, and dynamin II.

In summary, these observations suggest that the remarkable plasticity of tight junction structure that we have recently described<sup>4,34</sup> is essential for barrier maintenance during epithelial shedding. Although the cues that direct the observed junctional proliferation remain to be defined, the data suggest that they may be useful therapeutic targets for barrier maintenance in disease.

## Supplementary Material

Note: To access the supplementary material accompanying this article visit the online version of *Gastroenterology* at [www.gastrojournal.org](http://www.gastrojournal.org) and at doi: 10.1053/j.gastro.2011.01.004.

## References

- Farquhar M, Palade G. Junctional complexes in various epithelia. *J Cell Biol* 1963;17:375–412.
- Marchiando AM, Graham WV, Turner JR. Epithelial barriers in homeostasis and disease. *Annu Rev Pathol* 2010;5:119–144.
- Madara JL. Maintenance of the macromolecular barrier at cell extrusion sites in intestinal epithelium: physiological rearrangement of tight junctions. *J Membr Biol* 1990;116:177–184.
- Marchiando AM, Shen L, Graham WV, et al. Caveolin-1-dependent occludin endocytosis is required for TNF-induced tight junction regulation in vivo. *J Cell Biol* 2010;189:111–126.
- Schmitz H, Barmeyer C, Fromm M, et al. Altered tight junction structure contributes to the impaired epithelial barrier function in ulcerative colitis. *Gastroenterology* 1999;116:301–309.
- Gitter AH, Wullstein F, Fromm M, et al. Epithelial barrier defects in ulcerative colitis: characterization and quantification by electrophysiological imaging. *Gastroenterology* 2001;121:1320–1328.
- Rosenblatt J, Raff MC, Cramer LP. An epithelial cell destined for apoptosis signals its neighbors to extrude it by an actin- and myosin-dependent mechanism. *Curr Biol* 2001;11:1847–1857.
- Slattum G, McGee KM, Rosenblatt J. P115 RhoGEF and microtubules decide the direction apoptotic cells extrude from an epithelium. *J Cell Biol* 2009;186:693–702.
- Clayburgh DR, Barrett TA, Tang Y, et al. Epithelial myosin light chain kinase-dependent barrier dysfunction mediates T cell activation-induced diarrhea in vivo. *J Clin Invest* 2005;115:2702–2715.
- Watson AJ, Chu S, Sieck L, et al. Epithelial barrier function in vivo is sustained despite gaps in epithelial layers. *Gastroenterology* 2005;129:902–912.
- Kiesslich R, Goetz M, Angus EM, et al. Identification of epithelial gaps in human small and large intestine by confocal endomicroscopy. *Gastroenterology* 2007;133:1769–1778.
- Parkos CA, Colgan SP, Bacarra AE, et al. Intestinal epithelia (T84) possess basolateral ligands for CD11b/CD18-mediated neutrophil adherence. *Am J Physiol* 1995;268:C472–C479.
- Umeda K, Ikenouchi J, Katahira-Tayama S, et al. ZO-1 and ZO-2 independently determine where claudins are polymerized in tight-junction strand formation. *Cell* 2006;126:741–754.
- Yu D, Marchiando AM, Weber CR, et al. MLCK-dependent exchange and actin binding region-dependent anchoring of ZO-1 regulate tight junction barrier function. *Proc Natl Acad Sci U S A* 2010;107:8237–8241.
- Furuse M, Hata M, Furuse K, et al. Claudin-based tight junctions are crucial for the mammalian epidermal barrier: a lesson from claudin-1-deficient mice. *J Cell Biol* 2002;156:1099–1111.
- Macia E, Ehrlich M, Massol R, et al. Dynasore, a cell-permeable inhibitor of dynamin. *Dev Cell* 2006;10:839–850.

17. Amano M, Ito M, Kimura K, et al. Phosphorylation and activation of myosin by Rho-associated kinase (Rho-kinase). *J Biol Chem* 1996;271:20246–20249.
18. Ivanov AI, Bachar M, Babbin BA, et al. A unique role for non-muscle myosin heavy chain IIA in regulation of epithelial apical junctions. *PLoS One* 2007;2:e658.
19. Straight AF, Cheung A, Limouze J, et al. Dissecting temporal and spatial control of cytokinesis with a myosin II inhibitor. *Science* 2003;299:1743–1747.
20. Uehata M, Ishizaki T, Satoh H, et al. Calcium sensitization of smooth muscle mediated by a Rho-associated protein kinase in hypertension. *Nature* 1997;389:990–994.
21. Clayburgh DR, Rosen S, Witkowski ED, et al. A differentiation-dependent splice variant of myosin light chain kinase, MLCK1, regulates epithelial tight junction permeability. *J Biol Chem* 2004;279:55506–55513.
22. Hofmann C, Obermeier F, Artinger M, et al. Cell-cell contacts prevent anoikis in primary human colonic epithelial cells. *Gastroenterology* 2007;132:587–600.
23. Piguet PF, Vesin C, Guo J, et al. TNF-induced enterocyte apoptosis in mice is mediated by the TNF receptor 1 and does not require p53. *Eur J Immunol* 1998;28:3499–3505.
24. Caserta TM, Smith AN, Gultice AD, et al. Q-VD-OPh, a broad spectrum caspase inhibitor with potent antiapoptotic properties. *Apoptosis* 2003;8:345–352.
25. Bojarski C, Gitter AH, Bendfeldt K, et al. Permeability of human HT-29/B6 colonic epithelium as a function of apoptosis. *J Physiol* 2001;535:541–552.
26. Pentecost M, Otto G, Theriot JA, et al. *Listeria monocytogenes* invades the epithelial junctions at sites of cell extrusion. *PLoS Pathog* 2006;2:e3.
27. Baert FJ, D'Haens GR, Peeters M, et al. Tumor necrosis factor alpha antibody (infliximab) therapy profoundly down-regulates the inflammation in Crohn's ileocolitis. *Gastroenterology* 1999;116:22–28.
28. Strater J, Wedding U, Barth TF, et al. Rapid onset of apoptosis in vitro follows disruption of beta 1-integrin/matrix interactions in human colonic crypt cells. *Gastroenterology* 1996;110:1776–1784.
29. Wang F, Schwarz BT, Graham WV, et al. IFN-gamma-induced TNFR2 expression is required for TNF-dependent intestinal epithelial barrier dysfunction. *Gastroenterology* 2006;131:1153–1163.
30. Corredor J, Yan F, Shen CC, et al. Tumor necrosis factor regulates intestinal epithelial cell migration by receptor-dependent mechanisms. *Am J Physiol Cell Physiol* 2003;284:C953–C961.
31. Jin Y, Atkinson SJ, Marrs JA, et al. Myosin II light chain phosphorylation regulates membrane localization and apoptotic signaling of tumor necrosis factor receptor-1. *J Biol Chem* 2001;276:30342–30349.
32. Mandato CA, Bement WM. Actomyosin transports microtubules and microtubules control actomyosin recruitment during *Xenopus* oocyte wound healing. *Curr Biol* 2003;13:1096–1105.
33. Salazar MA, Kwiatkowski AV, Pellegrini L, et al. Tuba, a novel protein containing bin/amphiphysin/Rvs and Dbl homology domains, links dynamin to regulation of the actin cytoskeleton. *J Biol Chem* 2003;278:49031–49043.
34. Shen L, Weber CR, Turner JR. The tight junction protein complex undergoes rapid and continuous molecular remodeling at steady state. *J Cell Biol* 2008;181:683–695.

---

Received September 9, 2010. Accepted January 10, 2011.

#### Reprint requests

Address requests for reprints to: Jerrold R. Turner, MD, PhD, 5841 South Maryland, MC 1089, Chicago, Illinois 60637. e-mail: [jturner@bsd.uchicago.edu](mailto:jturner@bsd.uchicago.edu); or Alastair Watson, MD, Norwich Medical School, University of East Anglia, England. e-mail: [alastair.watson@uea.ac.uk](mailto:alastair.watson@uea.ac.uk).

#### Acknowledgments

L.S. and W.V.G. contributed equally to this work as second authors. J.R.T. and A.J.M.W. contributed equally to this work.

The authors thank V. Bindokas and Yimei Chen for confocal and electron microscopy support, respectively, and Danielle S. Smith for her outstanding efforts in cataloging and preparing data for analysis.

#### Conflicts of interest

The authors disclose no conflicts.

#### Funding

Supported by the National Institutes of Health (grants R01DK61931, R01DK68271, and P01DK67887 to J.R.T.), the University of Chicago Cancer Center (P30CA14599), T32HL007237 (to A.M.M.), the University of Chicago Institute for Translational Medicine (UL1RR024999), a Crohn's and Colitis Foundation of America research fellowship supported by Ms Laura McAteer Hoffman (to L.S.), and Wellcome Trust grant WT087768AIA (to A.J.M.W.).

## Supplementary Materials and Methods

### *Live Animal Imaging*

EGFP was imaged using an Argon laser with a spectral emission range of 490 to 568 nm, mRFP1 was imaged using a DPSS 561 laser with a spectral emission range of 577 to 679 nm, and Alexa 633 was imaged using an HeNe 633 laser; a pinhole of 200  $\mu\text{m}$  was used for all 3 fluorophores.<sup>1-3</sup> Hoechst dye was imaged using a multiphoton laser with a spectral emission range of 400 to 492 nm and pinhole of 600  $\mu\text{m}$ . Line scanning was performed at 200 or 700 Hz. Postacquisition image analysis was performed using MetaMorph 7 (Molecular Devices, Sunnyvale, CA).

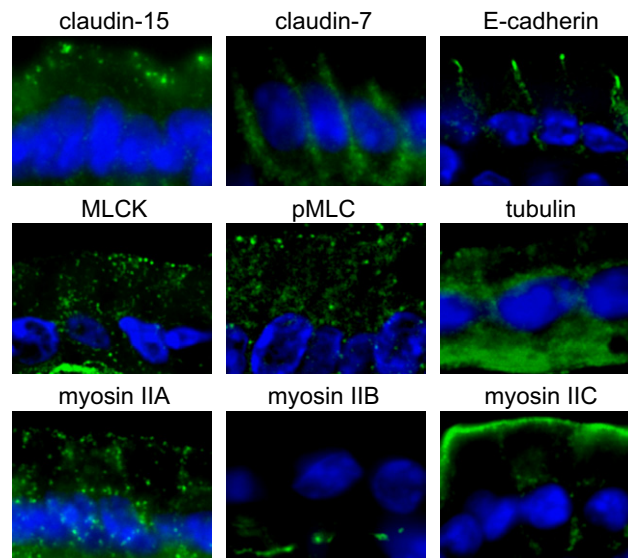
### *Immunofluorescence*

Mouse jejunum was snap frozen in OCT and stored at  $-80^{\circ}\text{C}$ . Frozen sections (10  $\mu\text{m}$ ) were fixed in 1% paraformaldehyde and immunostained as described previously using primary rabbit anti-[CE]-claudin-15 (Invitrogen, Carlsbad, CA), rat anti-E-cadherin (Invitrogen), monoclonal rat anti-ZO-1,<sup>4</sup> mouse monoclonal anti-occludin (Invitrogen), rabbit anti-ROCK (Cell Signaling Technology, Danvers, MA), rabbit anti-myosin IIA (Cell Signaling Technology), rabbit anti-myosin IIB (Cell Signaling Technology), rabbit anti-myosin IIC (Cell Signaling Technology), affinity-purified rabbit anti-phosphorylated MLC,<sup>5</sup> rabbit anti-cleaved caspase-3 (Cell Signaling Technology), mouse anti-tubulin (Zymed, San Francisco, CA), or mouse anti-MLCK (Sigma, St Louis, MO) primary antibodies and Alexa Fluor 488 or 594 conjugated sec-

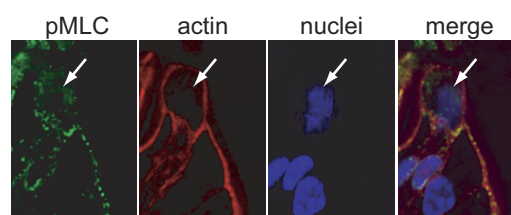
ondary antibodies (Invitrogen) along with Alexa Fluor 488 or 594 conjugated phalloidin (Invitrogen) and Hoechst 33342 (Invitrogen). Sections were mounted in Prolong Gold (Invitrogen), and imaging was performed using a DM4000 epifluorescence microscope (Leica Microsystems, Bannockburn, IL) equipped with 4',6-diamidino-2-phenylindole, Endow GFP, and Texas Red zero pixel shift filter sets (Chroma Technology Corp, Bellows Falls, VT), 63 $\times$  1.32 NA oil immersion objective or 20 $\times$  0.7 NA objective, and a Coolsnap HQ camera (Roper Scientific, Sarasota, FL) controlled by MetaMorph 7. Z-stacks were collected at 0.2- $\mu\text{m}$  or 1- $\mu\text{m}$  intervals and deconvolved using Autodeblur X2 (Media Cybernetics, Bethesda, MD) for 10 iterations.

### References

1. Watson AJ, Chu S, Sieck L, et al. Epithelial barrier function in vivo is sustained despite gaps in epithelial layers. *Gastroenterology* 2005;129:902-912.
2. Kiesslich R, Goetz M, Angus EM, et al. Identification of epithelial gaps in human small and large intestine by confocal endomicroscopy. *Gastroenterology* 2007;133:1769-1778.
3. Marchiando AM, Shen L, Graham WV, et al. Caveolin-1-dependent occludin endocytosis is required for TNF-induced tight junction regulation in vivo. *J Cell Biol* 2010;189:111-126.
4. Stevenson BR, Siliciano JD, Mooseker MS, et al. Identification of ZO-1: a high molecular weight polypeptide associated with the tight junction (Zonula Occludens) in a variety of epithelia. *J Cell Biol* 1986;103:755-766.
5. Berglund JJ, Riegler M, Zolotarevsky Y, et al. Regulation of human jejunal transmucosal resistance and MLC phosphorylation by Na<sup>+</sup>-glucose cotransport. *Am J Physiol Gastrointest Liver Physiol* 2001;281:G1487-G1493.



**Supplementary Figure 1.** Immunohistochemistry of claudin-15, claudin-7, E-cadherin, MLCK, phosphorylated MLC, tubulin, myosin IIA, myosin IIB, and myosin IIC (all in *green*) in jejunal enterocytes of untreated wild-type mice. Nuclei (*blue*) are shown for orientation.



**Supplementary Figure 2.** Wild-type mice were injected with 7.5  $\mu\text{g}$  TNF, and a segment of jejunum was perfused with 50  $\mu\text{mol/L}$  Q-VD-OPH and labeled for phosphorylated MLC (pMLC; *green*), actin (*red*), and nuclei (*blue*).